Journal of Computational Physics 228 (2009) 266–281

Contents lists available at ScienceDirect

Journal of Computational Physics

journal homepage: www.elsevier.com/locate/jcp

Efficient stochastic Galerkin methods for random diffusion equations

Dongbin Xiu *, Jie Shen

Department of Mathematics, Purdue University, 150 N. University Street, West Lafayette, IN 47907, USA

ARTICLE INFO

Article history:
Received 5 December 2007
Received in revised form 14 July 2008
Accepted 9 September 2008
Available online 18 September 2008

Keywords:
Generalized polynomial chaos
Stochastic Galerkin
Random diffusion
Uncertainty quantification

ABSTRACT

We discuss in this paper efficient solvers for stochastic diffusion equations in random media. We employ generalized polynomial chaos (gPC) expansion to express the solution in a convergent series and obtain a set of deterministic equations for the expansion coefficients by Galerkin projection. Although the resulting system of diffusion equations are coupled, we show that one can construct fast numerical methods to solve them in a *decoupled* fashion. The methods are based on separation of the diagonal terms and off-diagonal terms in the matrix of the Galerkin system. We examine properties of this matrix and show that the proposed method is unconditionally stable for unsteady problems and convergent for steady problems with a convergent rate independent of discretization parameters. Numerical examples are provided, for both steady and unsteady random diffusions, to support the analysis.

1. Introduction

We discuss in this paper simulations of diffusion problems with uncertainties. In general the uncertainties may enter through initial conditions, boundary conditions, or material properties. A representative example is flow through porous media, where the medium properties, e.g. permeability, are not precisely known due to lack of measurements and their accuracy. Here we discuss fast algorithms based on (generalized) polynomial chaos methods. Such methods have received considerable attention recently due to its efficiency in solving many stochastic problems. The original polynomial chaos (PC) method was developed by Ghanem and co-workers, cf. [9]. It was inspired by the Wiener chaos expansion which employs Hermite polynomials to represent Gaussian random processes [21]. Since its introduction, the PC method has been applied to many problems, including random diffusion [6–8,17]. Later the approach was extended to generalized polynomial chaos (gPC) where general orthogonal polynomials are adopted for improved representations of more general random processes [25]. With this extension different types of polynomials can be chosen to design efficient methods for problems with non-Gaussian inputs. Further extensions along this line include using piecewise basis functions to deal with discontinuity in random space more effectively [3,11,12,20].

With PC/gPC serving as a complete basis to represent random processes, a stochastic Galerkin projection can be used to transform the (stochastic) governing equations to a set of deterministic equations that can be readily discretized via standard numerical techniques, see, for example, Ref. [1,3,4,9,11,14,25,24,26]. Often such a procedure results in a set of *coupled* equations. For a stochastic diffusion equation this occurs when the diffusivity (or permeability, conductivity) is modeled as a random field. Here we employ the standard approach which models the random diffusivity field as a linear functional of finite number of (independent) random variables. The resulting deterministic equations from a Galerkin method are a set of coupled diffusion equations, which can be readily written in a vector/matrix form. We demonstrate that efficient algorithms can be constructed where only the diagonal terms are inverted whereas the off-diagonal terms are treated explicitly. This results

* Corresponding author. Tel.: +1 765 496 2846.
E-mail addresses: dxiu@math.purdue.edu (D. Xiu), shen@math.purdue.edu (J. Shen).

0021-9991/$ - see front matter © 2008 Elsevier Inc. All rights reserved.
doi:10.1016/j.jcp.2008.09.008

in a mixed explicit/implicit scheme for unsteady diffusion and a Jacobi iteration for steady diffusion. The important feature is that the system of equations are *decoupled* and existing methods for deterministic diffusion can be employed. Although such approaches have been used in practice, for both steady [24] and unsteady [27] random diffusions, their effectiveness has not been rigorously investigated. Here we show rigorously that the stiffness matrix of the Galerkin system, in the case of identical beta or gamma distributions, is strictly diagonally dominant which allows us to show that (i) a first-order mixed explicit/implicit scheme for unsteady diffusion problems is unconditionally stable; and (ii) the preconditioned CG method with a decoupled system as a preconditioner, and the simple Jacobi iterative scheme, converge at a rate which is independent of discretization parameters in the identical beta distribution case and only weakly dependent on the discretization parameters in the gamma distribution case.

It is also worth mentioning other means to decouple these random diffusion equations.

One approach is to employ the double-orthogonal polynomials [3] which can be applied when the random diffusivity is linear in terms of the input random variables (same as the case considered in this paper). The double-orthogonal polynomials, however, do not possess a hierarchical structure, and thus in multidimensional random spaces one needs to use tensor products of the univariate polynomials. This can increase computational cost drastically due to the fast growth in the number of basis functions.

Another approach is to use stochastic collocation methods (SC), which naturally leads to decoupled system of equations. Earlier attempts typically utilize tensor products of quadrature points, cf. [19]. Although it is still of high order, as shown in [2], the exponential growth of the number collocation points prevents its wide use in high dimensional random spaces. A more efficient alternative is to use Smolyak sparse grid [16], which was proposed in Ref. [23] and shown to be highly effectively for stochastic problems with high dimensional random inputs. In addition to solution statistics (e.g. mean and variance), a pseudo-spectral scheme can be employed to construct the complete gPC expansion [22].

Although the sparse grid based SC method is highly efficient, in general the number of (uncoupled) deterministic equations is larger than that of (coupled) equations from gPC Galerkin. This is particularly true at higher orders, as in large random dimensions the number of sparse grid SC equations scales as $\sim 2^P$ times the number of gPC Galerkin equations, where P is the order of approximation. Although adaptive choice of collocation nodes, based on solution property, can be made to reduce the computational cost [5], the number of equations can still be significantly higher than that of gPC Galerkin method, especially at high random dimensions and/or high-order expansions. Therefore it is important to develop efficient algorithms for the gPC Galerkin system which, albeit coupled, involves the "least" number of equations.

This paper is organized as follows. In Section 2 we formulate the random diffusion problem, for both steady and unsteady state problems. The gPC Galerkin method is presented in Section 3 where we prove a few important properties of the matrix structure. A mixed explicit/implicit algorithm is presented in Section 4, and its convergence and stability are established. We finally present numerical examples in Section 5.

2. Governing equations

We consider a time-dependent stochastic diffusion equation

$$\begin{aligned} &\tfrac{\partial u(t,x,y)}{\partial t} = \nabla_x \cdot (\kappa(x,y)\nabla_x u(t,x,y)) + f(t,x,y), \quad x \in \Omega, t \in (0,T]; \\ &u(0,x,y) = u_0(x,y), \quad u(t,\cdot,y)|_{\partial\Omega} = 0 \end{aligned} \tag{2.1}$$

and its steady state counterpart

$$-\nabla_x \cdot (\kappa(x,y)\nabla_x u(x,y)) = f(x,y), \quad x \in \Omega; \qquad u(\cdot,y)|_{\partial\Omega} = 0, \tag{2.2}$$

where $x = (x_1, \ldots, x_d)^T \in \Omega \subset \mathbb{R}^d, d = 1,2,3$, are the spatial coordinates, and $y = (y_1, \ldots, y_N) \in \mathbb{R}^N, N \geqslant 1$, is a random vector with independent and identically distributed components.

We assume that the random diffusivity field takes a form

$$\kappa(x,y) = \hat{\kappa}_0(x) + \sum_{i=1}^{N} \hat{\kappa}_i(x) y_i, \tag{2.3}$$

where $\{\hat{\kappa}_i(x)\}_{i=0}^N$ are fixed functions with $\hat{\kappa}_0(x) > 0, \forall x$. Alternatively (2.3) can be written as

$$\kappa(x,y) = \sum_{i=0}^{N} \hat{\kappa}_i(x) y_i, \tag{2.4}$$

where $y_0 = 1$.

For well-posedness we require

$$\kappa(x,y) \geqslant \kappa_{\min} > 0, \qquad \forall x \in \Omega, y \in \mathbb{R}^N. \tag{2.5}$$

Such a requirement obviously excludes random vector y that is unbounded from below, e.g. Gaussian distribution. Throughout this paper we will only consider random variables that are bounded from below.

3. GPC Galerkin method

3.1. GPC Galerkin equations

The Pth-order, gPC approximations of $u(t,x,y)$ and $f(t,x,y)$ are

$$u(t,x,y) \approx \sum_{m=1}^{M} \hat{\upsilon}_m(t,x)\Phi_m(y), \qquad f(t,x,y) \approx \sum_{m=1}^{M} \hat{f}_m(t,x)\Phi_m(y), \tag{3.1}$$

where $M = \binom{N+P}{N}$, $\{\Phi_m(y)\}$ are N-variate orthonormal polynomials of degree up to P. They are constructed as products of a sequence of univariate polynomials in each direction of $y_i, i = 1, \ldots, N$, i.e.

$$\Phi_m(y) = \phi_{m_1}(y_1), \ldots, \phi_{m_N}(y_N), \qquad m_1 + \cdots + m_N \leqslant P, \tag{3.2}$$

where m_i is the order of the univariate polynomials of $\phi(y_i)$ in the y_i direction for $1 \leqslant i \leqslant N$.

These univariate polynomials are orthonormal (upon proper scaling), i.e.

$$\int \phi_j(y_i)\phi_k(y_i)\rho_i(y_i)\mathrm{d}y_i = \delta_{jk}, \qquad 1 \leqslant i \leqslant N, \tag{3.3}$$

where δ_{jk} is the Kronecker delta function and $\rho_i(y_i)$ is the probability distribution function for random variable y_i. The type of the polynomials $\phi(y_i)$ is determined by the distribution of y_i. For example, Hermite polynomials are better suited for Gaussian distribution (the original PC expansion [9]), Jacobi polynomials are better for beta distribution, etc. For detailed discussion, see Ref. [25]. The polynomials also satisfy a three-term recurrence relation:

$$z\phi_k(z) = a_k\phi_{k+1}(z) + b_k\phi_k(z) + c_k\phi_{k-1}(z), \qquad k \geqslant 1, \tag{3.4}$$

with $\phi_0 = 1, \phi_{-1} = 0$.

For the N-variate basis polynomials $\{\Phi_m(y)\}$, each index $1 \leqslant m \leqslant M$ corresponds to a unique sequence $m_1, \ldots, m_N$, and they are also orthonormal

$$\mathbb{E}[\Phi_m(y)\Phi_n(y)] = \int \Phi_m(y)\Phi_n(y)\rho(y)\mathrm{d}y = \delta_{mn}, \tag{3.5}$$

where $\rho(y) = \Pi_{i=1}^{N}\rho_i(y_i)$.

Upon substituting (2.3) and the approximation (3.1) into the governing Eq. (2.1) and projecting the resulting equation onto the subspace spanned by the first M gPC basis polynomials, we obtain for all $k = 1, \ldots, M$,

$$\begin{aligned}\frac{\partial\hat{\upsilon}_k}{\partial t}(t,x) &= \sum_{i=0}^{N}\sum_{j=1}^{M}\nabla_x\cdot(\hat{\kappa}_i(x)\nabla_x\hat{\upsilon}_j)e_{ijk} + \hat{f}_k(t,x)\\ &= \sum_{j=1}^{M}\nabla_x\cdot(a_{jk}(x)\nabla_x\hat{\upsilon}_j) + \hat{f}_k(t,x),\end{aligned} \tag{3.6}$$

where

$$\begin{aligned}e_{ijk} &= \mathbb{E}[y_i\Phi_j\Phi_k] = \int y_i\Phi_j(y)\Phi_k(y)\rho(y)\mathrm{d}y, \quad 0 \leqslant i \leqslant N, \quad 1 \leqslant j,k \leqslant M,\\ a_{jk}(x) &= \sum_{i=0}^{N}\hat{\kappa}_i(x)e_{ijk}, \quad 1 \leqslant j,k \leqslant M.\end{aligned} \tag{3.7}$$

Alternatively, we can write

$$a_{jk}(x) = \mathbb{E}[\kappa\Phi_j\Phi_k] = \int \kappa(x,y)\Phi_j(y)\Phi_k(y)\rho(y)\mathrm{d}y, \quad 1 \leqslant j,k \leqslant M. \tag{3.8}$$

Note this is a more general expression which is valid for general random diffusivity models not restricted to the linear form in y (2.3).

Let us denote $\mathbf{v} = (\hat{\upsilon}_1, \ldots, \hat{\upsilon}_M)^T$, $\mathbf{f} = (\hat{f}_1, \ldots, \hat{f}_M)^T$ and $\mathbf{A}(x) = (a_{jk})_{1\leqslant j,k\leqslant M}$. By definition, $\mathbf{A} = \mathbf{A}^T$ is symmetric. The gPC Galerkin Eq. (3.6) can be written as

$$\begin{aligned}&\tfrac{\partial\mathbf{v}}{\partial t}(t,x) = \nabla_x\cdot[\mathbf{A}(x)\nabla_x\mathbf{v}] + \mathbf{f}, \quad (t,x) \in (0,T]\times\Omega,\\ &\mathbf{v}(0,x) = \mathbf{v}_0(x), \quad \mathbf{v}|_{\partial\Omega} = 0.\end{aligned} \tag{3.9}$$

This is a coupled system of diffusion equations, where $\mathbf{v}_0(x)$ is the gPC expansion coefficient vector obtained by expressing the initial condition of (2.1) in the form of (3.1).

Similarly, by removing the time variable t from the above discussion, we find that the gPC Galerkin approximation to (2.2) is

$$-\nabla_x\cdot[\mathbf{A}(x)\nabla_x\mathbf{v}] = \mathbf{f}, \quad x \in \Omega; \qquad \mathbf{v}|_{\partial\Omega} = 0. \tag{3.10}$$

This is a coupled system of elliptic equations.

3.2. Properties of the matrix $A(x)$

The following results are based on the conditions described above, i.e.,

- Diffusivity field $\kappa(x,y)$ is constructed by (2.4) and satisfies (2.5);
- The N-variate polynomials basis functions used in the solution expansion (3.1) are constructed via (3.2) and are orthonormal as in (3.5);
- The univariate polynomials in the constructions of (3.2) are orthonormal as in (3.3) and satisfy the three-term recurrence relation (3.4);
- The gPC Galerkin approximation of problem (2.1) (resp. (2.2)) results in a system of Eq. (3.9) (resp. (3.10)), where the symmetric matrix $\mathbf{A}(x)$ is defined by (3.7).

Under these conditions, we have

Theorem 3.1. *The matrix $\mathbf{A}(x)$ is positive definite for any $x \in \Omega$, following assumption (2.5).*

Proof 1. Let $\mathbf{b} = (\hat{b}_1, \ldots, \hat{b}_M)^T$ be an arbitrary non-zero real vector, and $b(y) = \sum_{j=1}^{M} \hat{b}_j \Phi_j(y)$ be a random variable constructed by the $\mathbf{b}$ vector. By using the definition of $a_{jk}(x)$ in (3.8), we immediately have, for any $x \in \Omega$

$$\begin{aligned}\mathbf{b}^T\mathbf{A}(x)\mathbf{b} &= \sum_{j=1}^{M}\sum_{k=1}^{M} \hat{b}_j a_{jk}(x)\hat{b}_k \\ &= \sum_{j=1}^{M}\sum_{k=1}^{M} \hat{b}_j \int \kappa(x,y)\Phi_j(y)\Phi_k(y)\rho(y)\mathrm{d}y\hat{b}_k \\ &= \int \kappa(x,y)b^2(y)\rho(y)\mathrm{d}y \\ &> 0,\end{aligned}$$

where the last inequality follows from (2.5). Note this result is valid for general form of diffusivity (3.8) and is not restricted to the linear form (2.4), as it only assumes (2.5). □

Lemma 3.2. *Each row of $\mathbf{A}(x)$ has at most $(2N+1)$ non-zero entries.*

Proof 2. From the definition of the matrix $\mathbf{A}(x)$ in (3.7), we obtain, for $1 \leqslant j,k \leqslant M$,

$$a_{jk}(x) = \hat{\kappa}_0(x)e_{0jk} + \sum_{i=1}^{N}\hat{\kappa}_i(x)e_{ijk} = \hat{\kappa}_0(x)\delta_{jk} + \sum_{i=1}^{N}\hat{\kappa}_i(x)\mathbb{E}[y_i\Phi_j(y)\Phi_k(y)]. \tag{3.11}$$

The first term in the above expression goes into the diagonal entries of matrix $\mathbf{A}(x)$.

By using the three-term recurrence relation (3.4), the second term becomes

$$\begin{aligned}&\mathbb{E}[y_i\Phi_j(y)\Phi_k(y)] = \mathbb{E}[y_i\phi_{j_1}(y_1),\ldots,\phi_{j_N}(y_N)\phi_{k_1}(y_1),\ldots,\phi_{k_N}(y_N)] \\ &= \int\cdots\int \phi_{j_1}(y_1)\ldots[a_{j_i}\phi_{j_i+1}(y_i) + b_{j_i}\phi_{j_i}(y_i) + c_{j_i}\phi_{j_i-1}(y_i)]\ldots\phi_{j_N}(y_N)\cdot\phi_{k_1}(y_1),\ldots,\phi_{k_N}(y_N)\prod_{i=1}^{N}\rho_i(y_i)\mathrm{d}y_1,\ldots,\mathrm{d}y_N \\ &= \delta_{j_1,k_1},\ldots,\left(a_{j_i}\delta_{j_i+1,k_i} + b_{j_i}\delta_{j_i,k_i} + c_{j_i}\delta_{j_i-1,k_i}\right),\ldots,\delta_{j_N,k_N} \\ &= a_{j_i}\mathbb{E}[\Phi_{j^{i+}}(y)\Phi_k(y)] + b_{j_i}\mathbb{E}[\Phi_j(y)\Phi_k(y)] + c_{j_i}\mathbb{E}[\Phi_{j^{i-}}(y)\Phi_k(y)] \\ &= a_{j_i}\delta_{j^{i+},k} + b_{j_i}\delta_{j,k} + c_{j_i}\delta_{j^{i-},k},\end{aligned} \tag{3.12}$$

where

$$\begin{aligned}\Phi_{j^{i+}}(y) &= \phi_{j_1}(y_1),\ldots,\phi_{j_i+1}(y_i),\ldots,\phi_{j_N}(y_N), \\ \Phi_{j^{i-}}(y) &= \phi_{j_1}(y_1),\ldots,\phi_{j_i-1}(y_i),\ldots,\phi_{j_N}(y_N).\end{aligned}$$

That is, the multivariate polynomial $\Phi_{j^{i+}}(y)$ (resp. $\Phi_{j^{i-}}(y)$) is the same as $\Phi_j(y)$ except the order of its univariate polynomial component in the ith direction is perturbed by +1 (resp. −1).

The above derivation shows that for any row of $\mathbf{A}(x)$, each term in the N-term summation of (3.11) has one contribution to the diagonal term, and two non-zero contributions to the off-diagonal entries. Therefore the maximum of number of non-zero entries in each row of $\mathbf{A}(x)$ is $(2N+1)$. □

Following the above derivation the diagonal terms of $\mathbf{A}$ are

$$a_{jj}(x) = \hat{\kappa}_0(x) + \sum_{i=1}^{N} \hat{\kappa}_i(x) b_{j_i}, \qquad 1 \leqslant j \leqslant M, \tag{3.13}$$

where j_i are the orders of the univariate polynomials in the directions of y_i for $1 \leqslant i \leqslant N$ of the N-variate polynomial basis $\Phi_j(y)$.

Lemma 3.3. *Assume that the random variables $y_i, 1 \leqslant i \leqslant N$, in (2.4) have either an identical beta distribution in $(-1,1)$ with $\rho(y_i) \sim (1-y_i)^\alpha (1+y_i)^\alpha$, or a gamma distribution in $(0,+\infty)$ with $\rho(y_i) \sim y_i^\alpha e^{-y_i}$, where $\alpha > -1$ and the scaling constants are omitted. Then, the matrices $\mathbf{A}(x)$ derived via the corresponding gPC basis are strictly diagonal dominant $\forall x \in \Omega$. More precisely, we have*

$$a_{jj}(x) \geqslant \kappa_{\min} + \sum_{k=1, k\neq j}^{M} |a_{jk}(x)|, \qquad 1 \leqslant j \leqslant M, \forall x \in \Omega. \tag{3.14}$$

Proof 3. We start with the beta distribution case where $\rho(y_i) \sim (1-y_i)^\alpha (1+y_i)^\alpha$ which corresponds to the ultra-spherical polynomials [25]. Since $y_i \in [-1,1]$, taking $y_i = \pm 1$ in (2.3), the condition (2.5) immediately implies that

$$\hat{\kappa}_0(x) \geqslant \kappa_{\min} + \sum_{i=1}^{N} |\hat{\kappa}_i(x)|, \qquad \forall x \in \Omega. \tag{3.15}$$

We recall that for ultra-spherical polynomials, the coefficients in their three-term recurrence satisfy (c.f., [18])

$$b_m = 0, \qquad a_m, c_m > 0, \qquad a_m + c_m = 1, \qquad m \geqslant 1.$$

Therefore, we derive from Lemma 3.2, (3.7) and (3.12) that the sum of off-diagonal terms satisfy

$$\sum_{k=1, k\neq j}^{M} |a_{jk}(x)| = \sum_{i=1}^{N} |\hat{\kappa}_i(x)|(a_{j_i} + c_{j_i}) = \sum_{i=1}^{N} |\hat{\kappa}_i(x)|.$$

On the other hand, we derive from (3.13) that

$$a_{jj}(x) = \hat{\kappa}_0(x) \qquad 1 \leqslant j \leqslant M. \tag{3.16}$$

Then, the inequality (3.14) follows from the above and (3.15).

Consider now the case of gamma distribution with $\rho(y_i) \sim y_i^\alpha e^{-y_i}$ which corresponds to generalized Laguerre polynomials [25]. Since $y \in [0,\infty)^N$, letting $y = 0$ and $y \to \infty$ in (2.3) together with (2.5) leads to

$$\begin{aligned} &\hat{\kappa}_0(x) \geqslant \kappa_{\min}, \qquad \forall x \in \Omega; \\ &\hat{\kappa}_i(x) > 0, \qquad 1 \leqslant i \leqslant N, \quad \forall x \in \Omega. \end{aligned} \tag{3.17}$$

We recall that for generalized Laguerre polynomials, the coefficients in their three-term recurrence relation are (c.f., [18])

$$a_m = -(m+1), \quad b_m = 2m + \alpha + 1, \quad c_m = -(m+\alpha). \tag{3.18}$$

Hence, we have $b_m > 0, \forall m$, (since $\alpha > -1$) and $a_m + c_m = -b_m$. We then derive from Lemma 3.2, (3.7), (3.12), and the above relations that the sum of the off-diagonal terms satisfies

$$\sum_{k=1, k\neq j}^{M} |a_{jk}(x)| = \sum_{i=1}^{N} |\hat{\kappa}_i(x)(a_{j_i} + c_{j_i})| = \sum_{i=1}^{N} \hat{\kappa}_i(x) b_{j_i}.$$

We conclude from the above, (3.17) and (3.13). □

Remark 3.1. It is an open question whether the above lemma holds for general beta distributions in $(-1,1)$ with $\rho(y_i) \sim (1-y_i)^\alpha (1+y_i)^\beta$, $\alpha \neq \beta$, $\alpha, \beta > -1$, although the numerical results in Section 5 (cf. Fig. 5.4) appear to indicate that the lemma holds for the general beta distributions as well.

We now establish a simple result which plays an important role in designing efficient schemes for (3.9) and (3.10).

Lemma 3.4. *Assume that a symmetric $M \times M$ matrix $\mathbf{A} = (a_{ij})$ satisfies*

$$a_{jj} \geqslant \kappa + \sum_{k=1, k\neq j}^{M} |a_{jk}|, \qquad j = 1, 2, \ldots, M \tag{3.19}$$

and set

$$\mathbf{D} = \mathrm{diag}(\mathbf{A}), \quad \mathbf{A} = \mathbf{D} + \mathbf{S}. \tag{3.20}$$

Then,

$$2|\mathbf{u}^T \mathbf{S} \mathbf{v}| \leqslant \mathbf{u}^t (\mathbf{D} - \kappa \mathbf{I}) \mathbf{u} + \mathbf{v}^t (\mathbf{D} - \kappa \mathbf{I}) \mathbf{v}, \quad \forall \mathbf{u}, \mathbf{v} \in \mathbb{R}^M \tag{3.21}$$

and

$$\kappa \mathbf{u}^T\mathbf{u} \leqslant \mathbf{u}^T\mathbf{A}\mathbf{u} \leqslant \mathbf{u}^T(2\mathbf{D} - \kappa\mathbf{I})\mathbf{u}, \quad \forall \mathbf{u} \in \mathbb{R}^M. \tag{3.22}$$

Proof 4. For any $\mathbf{u}, \mathbf{v} \in \mathbb{R}^M$, using (3.19) and the fact that $s_{ij} = s_{ji}$, we find

$$\begin{aligned} 2|\mathbf{u}^T\mathbf{S}\mathbf{v}| &= 2|\sum_{i,j=1}^{M} s_{ij}u_i v_j| \leqslant \sum_{i,j=1}^{M}(|s_{ij}|u_i^2 + |s_{ij}|v_j^2) \\ &\leqslant \sum_{i=1}^{M}(a_{ii} - \kappa)u_i^2 + \sum_{j=1}^{M}(a_{jj} - \kappa)v_j^2 \end{aligned}$$

which is exactly (3.21).

Now take $\mathbf{v} = \mathbf{u}$ in (3.21), we find

$$\mathbf{u}^T\mathbf{A}\mathbf{u} = \mathbf{u}^T\mathbf{D}\mathbf{u} + \mathbf{u}^T\mathbf{S}\mathbf{u} \leqslant \mathbf{u}^T\mathbf{D}\mathbf{u} + \mathbf{u}^T(\mathbf{D} - \kappa I)\mathbf{u} = \mathbf{u}^T(2\mathbf{D} - \kappa\mathbf{I})\mathbf{u},$$

and

$$\mathbf{u}^T\mathbf{A}\mathbf{u} \geqslant \mathbf{u}^T\mathbf{D}\mathbf{u} - |\mathbf{u}^T\mathbf{S}\mathbf{u}| \geqslant \mathbf{u}^T\mathbf{D}\mathbf{u} - \mathbf{u}^T(\mathbf{D} - \kappa\mathbf{I})\mathbf{u} = \kappa\mathbf{u}^T\mathbf{u}.$$

□

4. Numerical approaches

A disadvantage of the stochastic Galerkin method, as opposed to the stochastic collocation method, is that it leads to a coupled parabolic system (3.9) or elliptic system (3.10) for all components of $\mathbf{v}$. We shall show below that by taking advantage of the diagonal dominance of $\mathbf{A}$, one can efficiently solve the systems (3.9) and (3.10) as decoupled equations, similar to the stochastic collocation approach.

4.1. Time-dependent problem (3.9)

To avoid solving a coupled elliptic system at each time step, we propose a mixed explicit/implicit scheme for time integration of (3.9). More precisely, we write

$$\mathbf{A}(x) = \mathbf{D}(x) + \mathbf{S}(x), \tag{4.1}$$

where $\mathbf{D}(x)$ is the diagonal part and $\mathbf{S}(x)$ the off-diagonal part, and treat the diagonal terms in (3.9) implicitly and the off-diagonal ones explicitly. For example, a mixed Euler explicit/implicit scheme takes the following form

$$\frac{\mathbf{v}^{n+1} - \mathbf{v}^n}{\Delta t} - \nabla_x \cdot [\mathbf{D}(x)\nabla_x \mathbf{v}^{n+1}] = \nabla_x \cdot [\mathbf{S}(x)\nabla_x \mathbf{v}^n] + \mathbf{f}^{n+1}, \tag{4.2}$$

where $\mathbf{v}^n = \mathbf{v}(t_n, x)$, $\mathbf{f}^{n+1} = \int_{t_n}^{t_{n+1}} \mathbf{f}(t,x)\mathrm{d}t$ and Δt is the time step. Note that at each time step, the above scheme requires solving only a sequence of M decoupled elliptic equations.

Theorem 4.1. *Under the conditions in Lemma 3.3, the scheme (4.2) is unconditionally stable, and*

$$\|\mathbf{v}^k\|^2 + \sum_{j=0}^{k-1}\{\|\mathbf{v}^j - \mathbf{v}^{j-1}\|^2 + \kappa_{\min}\Delta t\|\nabla_x \mathbf{v}^j\|^2\} \leqslant C\Big(\|\mathbf{v}^0\|^2 + \Delta t(D(x)\nabla_x \mathbf{v}^0, \nabla_x \mathbf{v}^0) + \|\mathbf{f}\|^2_{L^2([0,T]\times\Omega)}\Big), \quad \forall k \leqslant [T/\Delta t],$$

where $\|\cdot\|^2 = \int_\Omega \|\cdot\|_{l2}^2 \mathrm{d}x$.

Proof 5. Taking the inner product, with respect to x in $L^2(\Omega)$, of (4.2) with $2\Delta t\mathbf{v}^{n+1}$ and integration by parts, using the identity $2(a-b,a) = |a|^2 - |b|^2 + |a-b|^2$ and (3.21), we find

$$\begin{aligned} &\|\mathbf{v}^{n+1}\|^2 - \|\mathbf{v}^n\|^2 + \|\mathbf{v}^{n+1} - \mathbf{v}^n\|^2 + 2\Delta t(\mathbf{D}(x)\nabla_x \mathbf{v}^{n+1}, \nabla_x \mathbf{v}^{n+1}) \\ &= 2\Delta t(\mathbf{S}(x)\nabla_x \mathbf{v}^n, \nabla_x \mathbf{v}^{n+1}) + 2\Delta t(\mathbf{f}^{n+1}, \mathbf{v}^{n+1}) \\ &\leqslant \Delta t(\mathbf{D} - \kappa_{\min}\mathbf{I})\nabla_x \mathbf{v}^n, \nabla_x \mathbf{v}^n + \Delta t(\mathbf{D} - \kappa_{\min}\mathbf{I})\nabla_x \mathbf{v}^{n+1}, \nabla_x \mathbf{v}^{n+1} + \Delta t\|\mathbf{f}^{n+1}\|^2 + \Delta t\|\mathbf{v}^{n+1}\|^2. \end{aligned}$$

Summing up the above inequality for $n = 0$ to $n = k-1$ and dropping some unnecessary positive terms, we find

$$\|\mathbf{v}^k\|^2 + \sum_{j=0}^{k-1}\{\|\mathbf{v}^j - \mathbf{v}^{j-1}\|^2 + \kappa_{\min}\Delta t(\|\nabla_x \mathbf{v}^j\|^2 + \|\nabla_x \mathbf{v}^{j+1}\|^2)\} \leqslant \|\mathbf{v}^0\|^2 + \Delta t(\mathbf{D}(x)\nabla_x \mathbf{v}^0, \nabla_x \mathbf{v}^0) + \|\mathbf{f}\|^2_{L^2([0,T]\times\Omega)}.$$

□

Scheme (4.2) is only first order in time. For higher temporal accuracy, a high-order backward differentiation formula can be used [27]

$$\frac{\gamma_0 \mathbf{v}^{n+1}(x) - \sum_{q=0}^{J-1} \alpha_q \mathbf{v}^{n-q}(x)}{\Delta t} - \nabla_x \cdot [\mathbf{D}(x) \nabla_x \mathbf{v}^{n+1}] = \sum_{q=0}^{J-1} \beta_q \nabla_x \cdot [\mathbf{S}(x) \nabla_x \mathbf{v}^{n-q}] + \mathbf{f}^{n+1}, \tag{4.3}$$

where J is the order of accuracy in time. The coefficients in the scheme are listed in Table 4.1 for different temporal orders. It is unlikely that the above scheme will be unconditionally stable for $J \geqslant 2$, but one can expect the scheme with $J \geqslant 2$ to be stable under mild stability constraints.

Remark 4.1. In the decoupled system of Eqs. (4.2) or (4.3), the explicit evaluation of $\nabla_x \cdot [\mathbf{S} \nabla_x \mathbf{v}]$ can be accomplished by a matrix-vector product operation. Since $\mathbf{A}(x)$ is symmetric and only has $(2N+1)$ non-zero entries per row (see Lemma 3.2) for each component of the explicit term, the dominant computational cost is the evaluation of $(N+1)$ products which depends only on the random dimensionality N.

4.2. Steady state problem (3.10)

For the steady state problem (3.10), we shall treat the identical beta distributions and gamma distributions separately. For the identical beta distributions, we assume

$$\kappa_0(x) \leqslant \kappa_{\max} < +\infty, \qquad \forall x. \tag{4.4}$$

Using the same notations as in Lemma 3.4 and taking $y = 0$ in (2.3), we immediately derive from (4.4) and (3.16) that

$$\mathbf{u}^T \mathbf{D} \mathbf{u} = \hat{\kappa}_0(x) \mathbf{u}^T \mathbf{u} \leqslant \kappa_{\max} \mathbf{u}^T \mathbf{u}, \quad \forall x \in \Omega, \mathbf{u} \in \mathbb{R}^M. \tag{4.5}$$

We then derive from the above and (3.22) that

$$\kappa_{\min} \mathbf{u}^T \mathbf{u} \leqslant \mathbf{u}^T \mathbf{A}(x) \mathbf{u} \leqslant (2\kappa_{\max} - \kappa_{\min}) \mathbf{u}^T \mathbf{u}, \quad \forall x \in \Omega, \mathbf{u} \in \mathbb{R}^M. \tag{4.6}$$

Let us consider now (3.10) and define a bilinear form

$$a(\mathbf{u}, \mathbf{v}) = (\mathbf{A}(x) \nabla_x \mathbf{u}, \nabla_x \mathbf{v}), \quad \forall \mathbf{u}, \mathbf{v} \in H_0^1(\Omega)^M. \tag{4.7}$$

Then, we derive from (4.6) that

$$\kappa_{\min} (\nabla_x \mathbf{u}, \nabla_x \mathbf{u}) \leqslant a(\mathbf{u}, \mathbf{v}) \leqslant (2\kappa_{\max} - \kappa_{\min}) (\nabla_x \mathbf{u}, \nabla_x \mathbf{u}), \quad \forall \mathbf{u} \in H_0^1(\Omega)^M. \tag{4.8}$$

This inequality indicates that for the case with identical beta distributions the bilinear form associated with the Laplace operator $(\nabla_x \mathbf{u}, \nabla_x \mathbf{u})$ is an optimal preconditioner for $a(\mathbf{u}, \mathbf{v})$. In particular, this implies that the convergence rate of the preconditioned conjugate gradient (PCG) iteration, using the Laplace operator (with homogeneous Dirichlet boundary conditions) as a preconditioner, will be independent of discretization parameters.

Now we consider the case of gamma distributions. We shall make an additional assumption (which is not restrictive from a practical point of view):

$$\kappa_0(x), \hat{\kappa}_i(x) (i = 1, \ldots, N) \leqslant \kappa_{\max} < +\infty, \qquad \forall x. \tag{4.9}$$

Then, we derive from (4.9), (3.13), $b_m = 2m + \alpha + 1$ and $m_1 + \cdots + m_N \leqslant P$ that

$$a_{jj}(x) \leqslant \kappa_{\max} + \kappa_{\max} \sum_{i=1}^{N} (2j_i + \alpha + 1) = \kappa_{\max} + \kappa_{\max} \left(2 \sum_{i=1}^{N} j_i + N(\alpha + 1) \right) \leqslant (2P + N(\alpha + 1) + 1) \kappa_{\max}. \tag{4.10}$$

where N is the dimension of the random space and P is the highest polynomial order. Therefore, the same argument as above leads to

$$\kappa_{\min} (\nabla_x \mathbf{u}, \nabla_x \mathbf{u}) \leqslant a(\mathbf{u}, \mathbf{v}) \leqslant (2(2P + N(\alpha + 1) + 1) \kappa_{\max} - \kappa_{\min}) (\nabla_x \mathbf{u}, \nabla_x \mathbf{u}). \tag{4.11}$$

Table 4.1
Coefficients in the mixed explicit/implicit integration (4.3) (see, for example, Ref. [10], Chapter 8)

Coefficient	First order	Second order	Third order
γ_0	1	3/2	11/6
α_0	1	2	3
α_1	0	−1/2	−3/2
α_2	0	0	1/3
β_0	1	2	3
β_1	0	−1	−3
β_2	0	0	1

This result indicates that, in the case of gamma distributions, the convergence rate of the PCG iteration will depend on N and P weakly. This is consistent with the numerical results in Section 5.

By taking into account (3.21), it is also easy to see that the above conclusion also holds for the simple Jacobi iteration

$$-\nabla_x \cdot [\mathbf{D}(x)\nabla_x \mathbf{v}^{i+1}] = \nabla_x \cdot [\mathbf{S}(x)\nabla_x \mathbf{v}^i] + \mathbf{f} \tag{4.12}$$

which, in the case of identical beta distributions, is equivalent to

$$-\nabla_x \cdot [\kappa_0(x)\nabla_x \mathbf{v}^{i+1}] = \nabla_x \cdot \left[(\mathbf{A}(x) - \kappa_0(x))\nabla_x \mathbf{v}^i\right] + \mathbf{f}. \tag{4.13}$$

Notice that only one matrix inversion is needed for all components of $\mathbf{v}$. However, in the case of gamma distributions, (4.12) with full diagonal terms involves a matrix inversion for each component of $\mathbf{v}$. The numerical results in Section 5 (cf., Fig. 5.7) indicate that the iterative scheme (4.12) with full diagonal terms is much more robust than the scheme (4.13).

4.3. Advection–diffusion problem

The algorithm presented here can be extended to stochastic advection–diffusion problem in a straightforward manner. Let us consider, for example, the following equation

$$u_t + c(x) \cdot \nabla_x u = \nabla_x \cdot (\kappa(x,y)\nabla_x u) + f(t,x,y), \quad x \in \Omega, t \in (0,T], y \in \mathbb{R}^N, \tag{4.14}$$

where $c(x)$ is a deterministic advection velocity field, and proper initial and boundary conditions are imposed. We remark that the case of random advection velocity has been discussed extensively in literature, see, for example, Ref. [9]. Using the same notations and approach from above, the first-order (in time) mixed explicit/implicit scheme can be written as

$$\frac{\mathbf{v}^{n+1} - \mathbf{v}^n}{\Delta t} - \nabla_x \cdot [\mathbf{D}(x)\nabla_x \mathbf{v}^{n+1}] = -c \cdot \nabla \mathbf{v}^n + \nabla_x \cdot [\mathbf{S}(x)\nabla_x \mathbf{v}^n] + \mathbf{f}^{n+1}. \tag{4.15}$$

Similarly, a higher-order temporal scheme can be written in a similar fashion as that of (4.3),

$$\tfrac{1}{\Delta t}\left[\gamma_0 \mathbf{v}^{n+1}(x) - \sum_{q=0}^{J-1} \alpha_q \mathbf{v}^{n-q}(x)\right] - \nabla_x \cdot [\mathbf{D}(x)\nabla_x \mathbf{v}^{n+1}] = \mathbf{f}^{n+1} + \sum_{q=0}^{J-1} \beta_q(-c \cdot \nabla \mathbf{v}^{n-q} + \nabla_x \cdot [\mathbf{S}(x)\nabla_x \mathbf{v}^{n-q}]), \tag{4.16}$$

where the coefficients α, β are tabulated in Table 4.1.

5. Numerical examples

In this section we present numerical examples to support the analysis. The focus is on the discretization of random spaces and the convergence properties of the proposed schemes. Therefore all numerical examples are in one-dimensional physical space. Extensions to two and three dimensional spaces are straightforward. We also remark that the decoupling methods discussed here have been applied in practice, cf., [24,27], where extensive numerical tests were conducted for problems involving complex geometry and large random perturbation.

5.1. Steady state problem

We first consider the following problem in one spatial dimension ($d = 1$) and N(>1) random dimensions.

$$-\frac{\partial}{\partial x}\left[\kappa(x,y)\frac{\partial u}{\partial x}(x,y)\right] = f, \qquad (x,y) \in (0,1) \times \mathbb{R}^N \tag{5.1}$$

with forcing term $f = \text{const}$ and boundary conditions

$$u(0,y) = 0, \qquad u(1,y) = 0, \qquad y \in \mathbb{R}^N.$$

We assume that the random diffusivity has the form

$$\kappa(x,y) = 1 + \sigma \sum_{k=1}^{N} \frac{1}{k^2\pi^2} \cos(2\pi k x) y_k, \tag{5.2}$$

where $y = (y_1, \ldots, y_N)$ is a random vector with independent and identically distributed components. The form of (5.2) is similar to those obtained from a Karhunen–Loève expansion [13] with eigenvalues delaying as $1/k^4$. Here we employ (5.2) in order to eliminate the errors associated with a numerical Karhunen–Loève solver and to keep the random diffusivity strictly positive because the series converges as $N \to \infty$.

The spatial discretization is a p-type spectral element with high-order modal expansions utilizing Jacobi polynomials [10]. In all of the following computations, sufficiently high-order expansions are employed such that the spatial errors are negligible.

5.1.1. Random inputs with beta distribution

We first examine the case when the random variables in y have bounded support. In particular, we first set y as uniform random vector in $(-1,1)^N$ In the first example we set $N = 2$ and $\sigma = 1$ in (5.2). Since analytical solution is not readily available, we employ a well-resolved solution with gPC order $P = 8$ as the "exact" solution and examine convergence of errors at lower order gPC expansions. In Fig. 5.1 the errors in standard deviation (STD), with L^2 norm in x, are shown. Fast (exponential) error convergence is observed as the order of gPC expansion is increased, before machine accuracy is reached. For the iterative solver (4.12), its convergence criterion is set at 1×10^{-10}. Convergence can be reached in six steps of iterations, as shown in Fig. 5.2, for all orders of gPC solvers. More importantly, the convergence rate of the Jacobi iterative solvers is independent to the gPC expansion order.

Next we vary the dimensionality of the random inputs, i.e., N in (5.2). Computations are conducted for random dimensions as high as $N = 30$, which results in $M = 496$ gPC expansion terms at second-order ($P = 2$). Numerical experiments indicate that the convergence rate of the Jacobi iteration is independent of the random dimension N, as shown in Fig. 5.3.

Even though the diagonal dominance proof in Theorem 3.3 applies only to the symmetric beta distributions with $\alpha = \beta$, we examine the convergence properties numerically for general beta distribution with $\alpha \neq \beta$. The results are plotted in

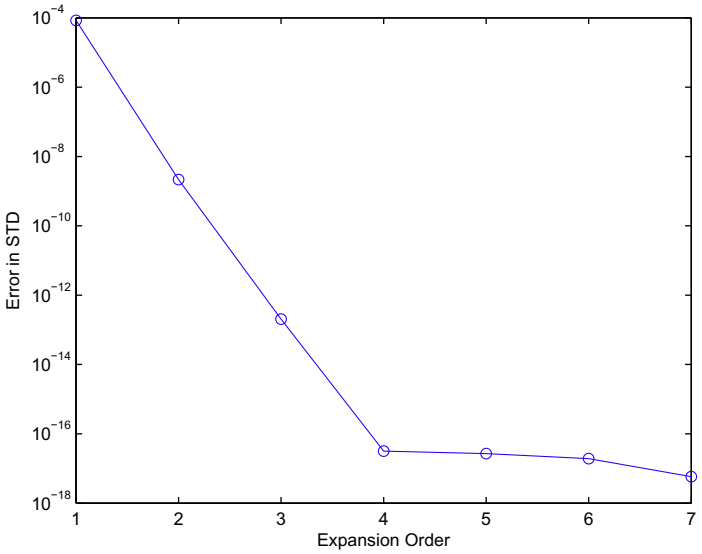

Fig. 5.1. Convergence of error in standard deviation (STD) for steady state diffusion computation with $N = 2$, $\sigma = 1$.

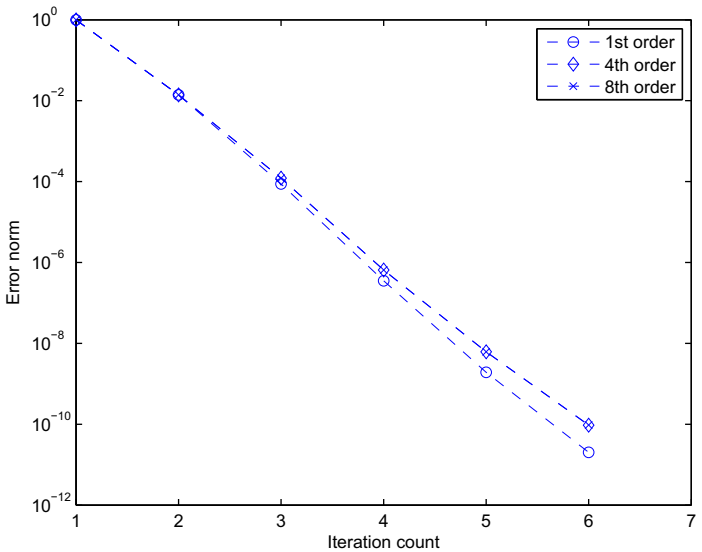

Fig. 5.2. Convergence of error norm in term of iterations for the steady state diffusion computation with $N = 2$, $\sigma = 1$.

Fig. 5.4, for various combinations of α, β, dimensionality N, and gPC order P. It can be seen that the convergence rate of the iterative solver is insensitive of the parameter values.

5.1.2. Random inputs with gamma distribution

Next we assume $\{y_k\}_{k=1}^N$ in the diffusivity model (5.2) have a gamma distribution with $\alpha = 1$ (see Lemma 3.3) and examine the performance of the iterative scheme (4.12). To ensure positiveness of the diffusivity we slightly change the form from (5.2) to

$$\kappa(x,y) = 1 + \sigma \sum_{k=1}^{N} \frac{1}{k^2\pi^2}[1 + \cos(2\pi k x)]y_k.$$

The results are shown in Fig. 5.5 with $N = 2$. It is clear that the convergence is again fast and its rate appears to be insensitive to the order of gPC expansion at higher orders.

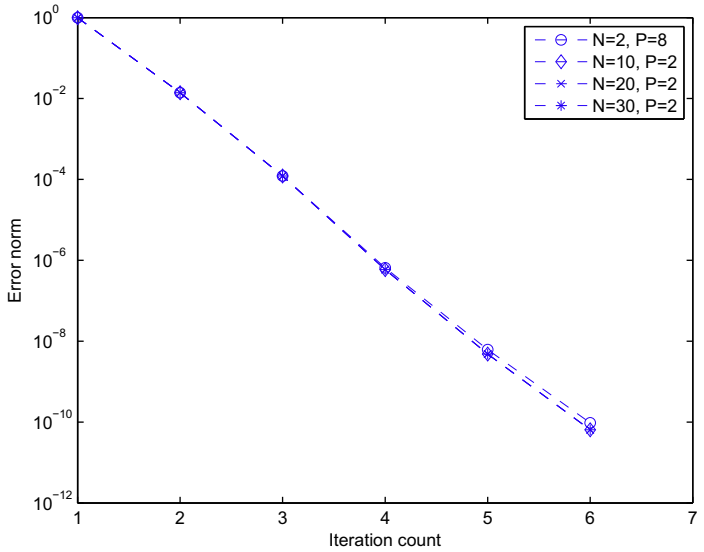

Fig. 5.3. Convergence of error norm in term of iterations for steady state diffusion computations with various random dimensions N.

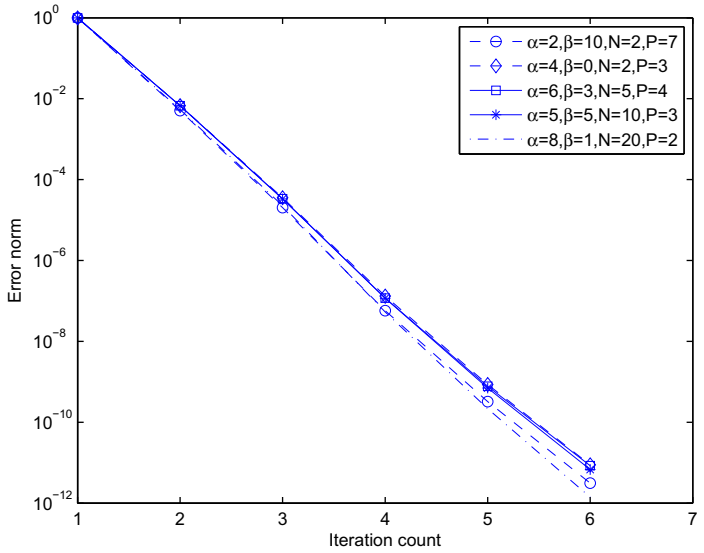

Fig. 5.4. Convergence of error norm in term of iterations for steady state diffusion computations with beta random inputs.

On the contrary, if one employs the iterative scheme based on the zeroth mode of the diffusivity field in (4.13), then the convergence becomes sensitive to the expansion order. This is shown in Fig. 5.6, where for higher-order expansions the convergence rate deteriorates. The comparison of the two iterative schemes is in Fig. 5.7, where it is clear that the proper scheme (4.12) is more robust and accurate than the iteration based on mean field (4.13).

5.2. Unsteady state problem

Here we consider a time-dependent version of problem (5.1)

$$\frac{\partial u}{\partial t} = \frac{\partial}{\partial x}\left[\kappa(x,y)\frac{\partial u}{\partial x}(x,y)\right] + f, \qquad (x,y) \in (0,1)\times\mathbb{R}^N, \tag{5.3}$$

where zero initial condition is prescribed and κ, f and boundary conditions are the same as those in (5.1) with y uniformly distributed in $(-1,1)^N$. Sufficiently high-order gPC is employed so that we can examine the errors induced by temporal dis-

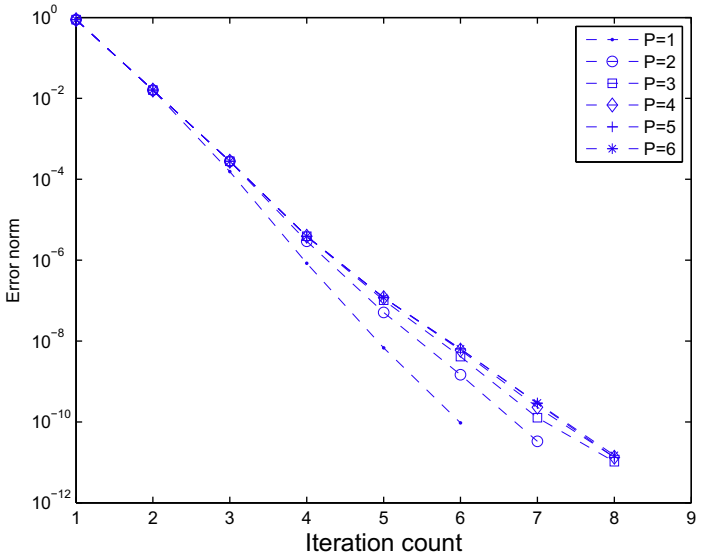

Fig. 5.5. Convergence of error norm for steady state diffusion with gamma random inputs ($N = 2$, $\alpha = 1$).

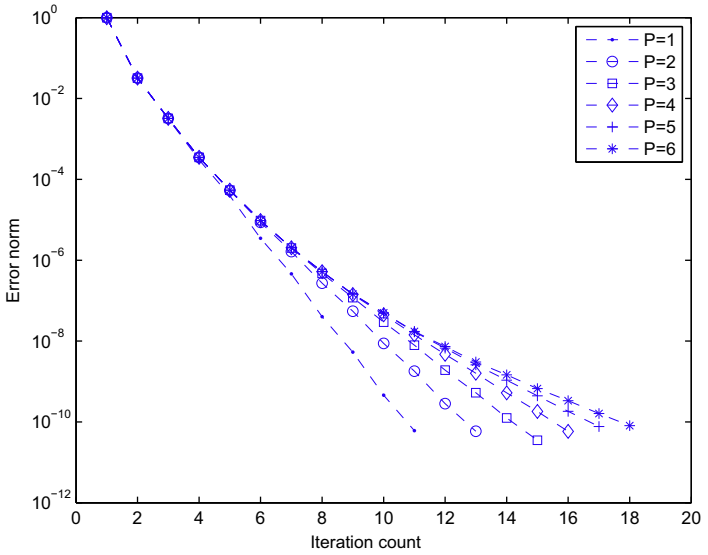

Fig. 5.6. Convergence of error norm for steady state diffusion with gamma random inputs by mean field iteration (4.13) ($N = 2$, $\alpha = 1$).

cretization. In Fig. 5.8 the errors in the standard deviation of the solution are reported at $T = 1$ with various sizes of time steps using the second-order explicit/implicit scheme (4.3). We observe that the scheme is stable for the whole range of time steps considered here and the error converges at an expected rate of two.

5.3. Advection–diffusion problem in random media

Finally we demonstrate the effectiveness of the algorithm via the stochastic advection–diffusion problem (4.14). Here the transport velocity is fixed as $c(x) = 1$, and no source term is introduced ($f = 0$). The length of the domain is $L = 10$ with $x \in [-5, 5]$. The diffusivity field is modeled as

$$\kappa(x, y) = \bar{\kappa}\left(1 + \sigma \sum_{i=1}^{N} \sqrt{\lambda_i} g_i(x) y_i\right), \tag{5.4}$$

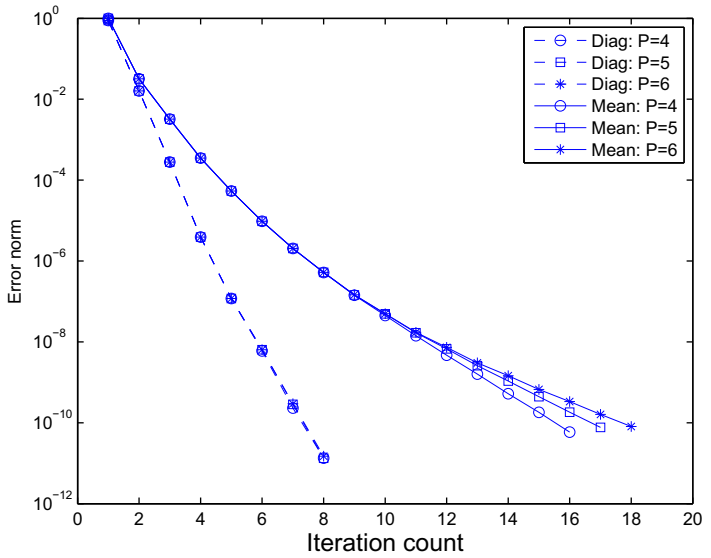

Fig. 5.7. Comparison of the convergence of iterations for steady state diffusion with gamma random inputs with $N = 2$, $\alpha = 1$. 'Diag' stands for iteration with the proper diagonal terms (4.12); and 'Mean' stands for iteration with the mean field (4.13).

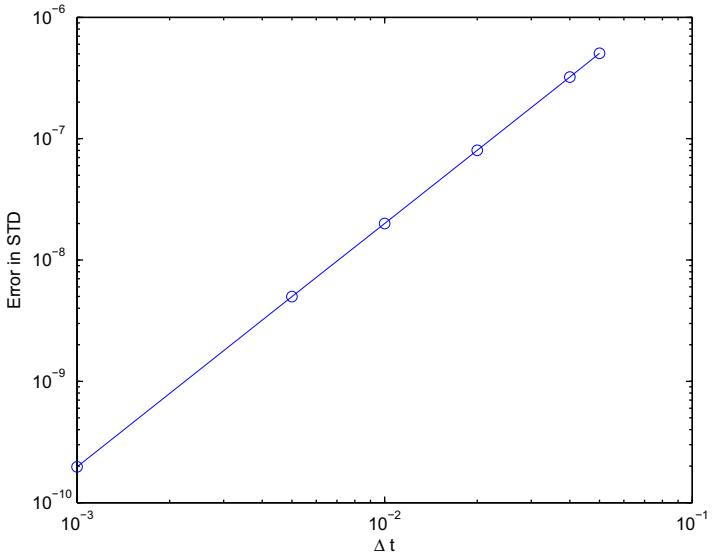

Fig. 5.8. Errors in standard deviation at $T = 1$ with different sizes of time step Δt.

where $\bar{\kappa} = 0.01$ is the mean diffusivity, $\sigma = 0.1$, $\{y_i\}$ are independent random variables uniformly distributed in $(-1, 1)$, and $\{\lambda_i, g_i(x)\}$ are the eigenvalues and eigenfunctions for

$$\int C(x,z)g_i(z)\mathrm{d}z = \lambda_i g_i(x), \qquad i = 1, 2, \ldots$$

where $C(x,z) = \exp(-\mid x - z \mid /\ell)$ is the covariance function for $\kappa(x,y)$ taking the exponential form with a correlation length ℓ. This is the widely adopted Karhunen–Loève expansion for random field [13]. Here we employ a short correlation length $\ell = 0.5$, compared to the length of the domain $L = 10$. On the left of Fig. 5.9 the decay of eigenvalues are shown. Based on the decay, we employ the first 20 eigenvalues and set $N = 20$ so that more than 95% of the total spectrum is retained. A few sample realizations of the 20-term construction (5.4) are shown in the right of Fig. 5.9, where the magnitude of the diffusivity field is scaled to order one for better visualization. The relatively rough structure of the random field can be clearly observed. For a rigorous analysis on the properties of numerical Karhunen–Loève expansion, see Ref. [15].

Two sets of boundary and initial conditions are used. One models the propagation of a front

$$u(-5,y,t) = 1, \quad u(5,y,t) = 0, \quad u(x,y,0) = \frac{1}{2}(1 - \tanh((x - x_0)/\delta)) \tag{5.5}$$

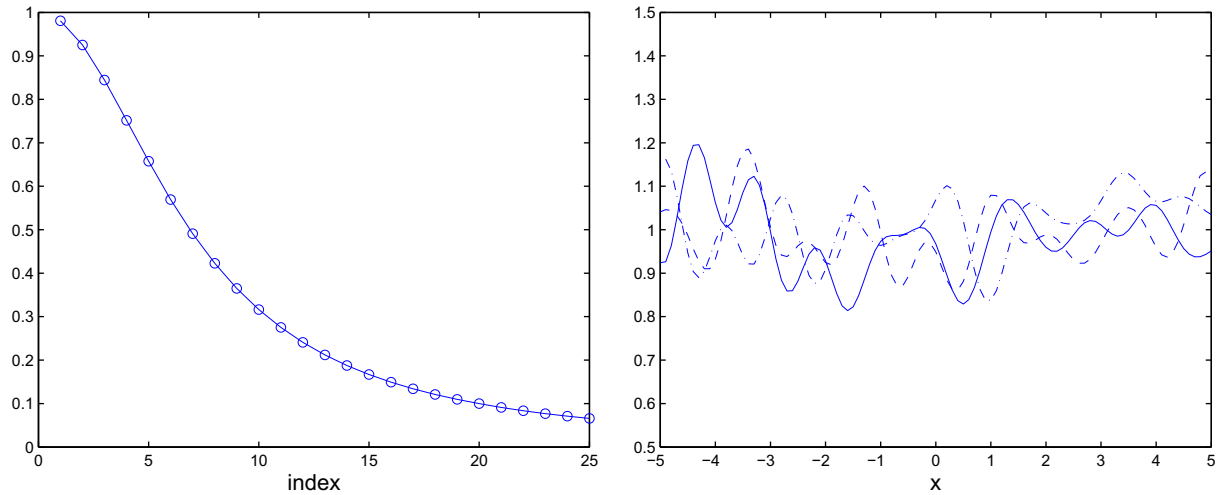

Fig. 5.9. Construction of the random diffusivity field (5.4) with correlation length 0.5. Left: eigenvalues of Karhunen–Loève expansion. Right: sample realizations of the diffusivity field with $N = 20$.

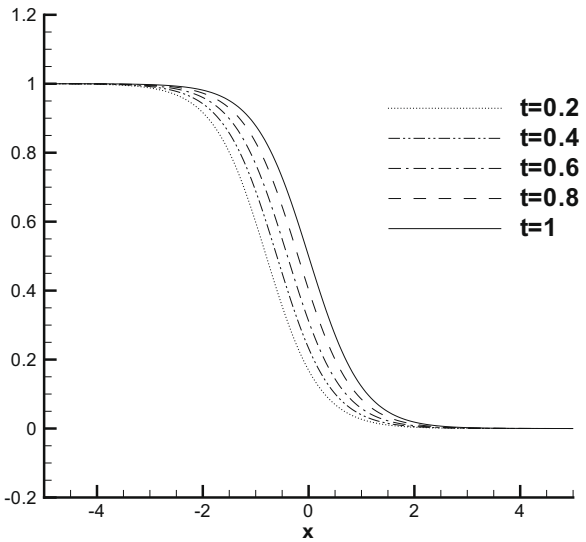

Fig. 5.10. Time evolution of the mean solution with the initial condition (5.5).

with $\delta = 1$, and the other models the propagation of a concentration

$$u(-5,y,t) = 0, \quad u(5,y,t) = 0, \quad u(x,y,0) = \frac{1}{\sqrt{2\pi}} e^{-(x-x_0)^2/\eta^2} \tag{5.6}$$

with $\eta = 0.5$. In both cases the initial conditions are centered at $x_0 = -1$ and the solutions are propagated up to $T = 1$. The second-order mixed explicit/implicit scheme (4.16) is employed with $\Delta t = 0.005$. The spatial discretization is the modal-type spectral/hp element method [10] with 10 elements, each one of twelfth order.

The time evolution of the mean solution and its standard deviations for the propagation of the front (5.5) are shown in Figs. 5.10 and 5.11. The uncertainty in the solution, measured by the standard deviation, follows the center of the mean profile and grows and widens as the solution is propagated to the right.

Similarly, the mean and standard deviation of the propagation of the concentration (5.6) are shown in Figs. 5.12 and 5.13. In this case the standard deviation exhibits multi-peak behavior, with one peak at the center of the mean solution and two smaller peaks at the front and end of the mean profile. The multi-peak standard deviation again grows and widens as the

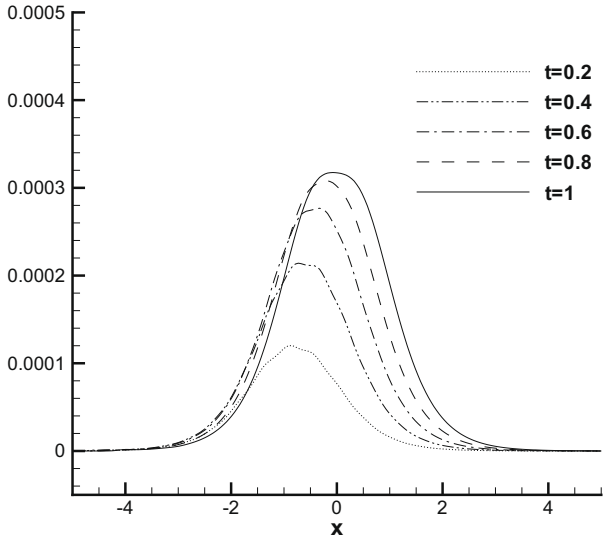

Fig. 5.11. Time evolution of the standard deviation of the solution with the initial condition (5.5).

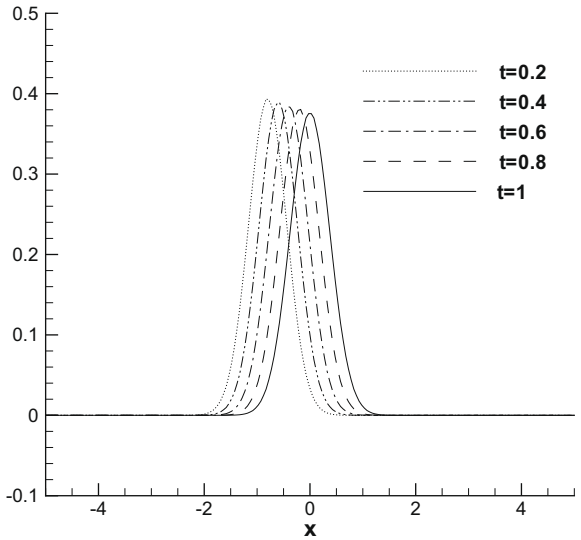

Fig. 5.12. Time evolution of the mean solution with the initial condition (5.6).

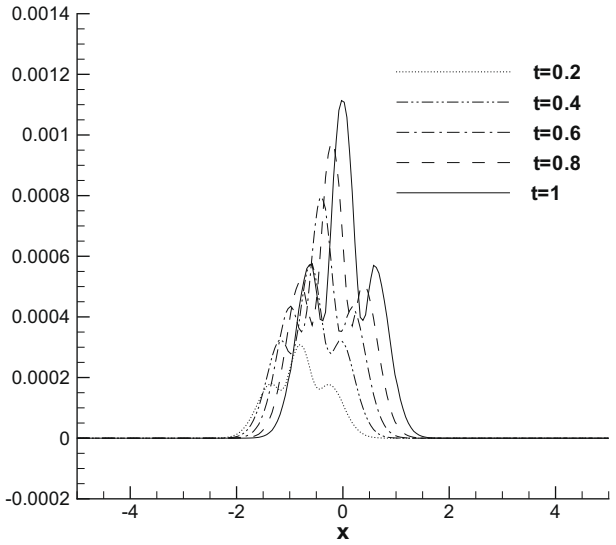

Fig. 5.13. Time evolution of the standard deviation of the solution with the initial condition (5.6).

solution is propagated downstream. Similar multi-peak structure in standard deviation has been observed in wave propagation in a random environment [28].

6. Summary

We presented in this paper efficient numerical methods for solutions of stochastic diffusion equations via the generalized polynomial chaos (gPC) Galerkin method. The proposed algorithms require only solutions of decoupled deterministic diffusion equations, and thus allow one to apply existing deterministic solvers. For unsteady problems, we proved that the first-order mixed explicit/implicit scheme is unconditionally stable while higher-order schemes are expected to be stable under mild constraints; for steady state problems, we showed that the convergence rate of the PCG iteration with Laplace preconditioner and the simple Jacobi iteration is independent of discretization parameters in the identical beta distribution case and weakly dependent on the discretization parameters in the gamma distribution case. Numerical examples were provided to verify the theoretical findings and demonstrate the effectiveness of the algorithm. The proposed algorithms provide a competitive alternative for stochastic collocation methods.

Acknowledgments

The work of D. Xiu is supported in part by AFOSR (Air Force Office of Scientific Research) Grant FA9550-08-1-0353 and NSF CAREER Award DMS-0645035. The work of J. Shen is supported in part by AFOSR Grant FA9550-08-1-0416 and NSF DMS-0610646.

References

[1] S. Acharjee, N. Zabaras, Uncertainty propagation in finite deformations – a spectral stochastic Lagrangian approach, Comput. Meth. Appl. Math. Eng. 195 (2006) 2289–2312.
[2] I. Babuška, F. Nobile, R. Tempone, A stochastic collocation method for elliptic partial differential equations with random input data, SIAM J. Num. Anal. 45 (3) (2007) 1005–1034.
[3] I. Babuška, R. Tempone, G.E. Zouraris, Galerkin finite element approximations of stochastic elliptic differential equations, SIAM J. Num. Anal. 42 (2004) 800–825.
[4] P. Frauenfelder, Ch. Schwab, R.A. Todor, Finite elements for elliptic problems with stochastic coefficients, Comput. Meth. Appl. Mech. Eng. 194 (2005) 205–228.
[5] B. Ganapathysubramanian, N. Zabaras, Sparse grid collocation schemes for stochastic natural convection problems, J. Comput. Phys. 225 (1) (2007) 652–685.
[6] R.G. Ghanem, Scales of fluctuation and the propagation of uncertainty in random porous media, Water Resour. Res. 34 (1998) 2123.
[7] R.G. Ghanem, Ingredients for a general purpose stochastic finite element formulation, Comput. Methods Appl. Mech. Eng. 168 (1999) 19–34.
[8] R.G. Ghanem, Stochastic finite elements for heterogeneous media with multiple random non-Gaussian properties, ASCE J. Eng. Mech. 125 (1) (1999) 26–40.
[9] R.G. Ghanem, P. Spanos, Stochastic Finite Elements: A Spectral Approach, Springer-Verlag, 1991.
[10] G.E. Karniadakis, S.J. Sherwin, Spectral/hp Element Methods for CFD, Oxford University Press, 1999.
[11] O. Le Maitre, O. Knio, H. Najm, R. Ghanem, Uncertainty propagation using Wiener–Haar expansions, J. Comput. Phys. 197 (2004) 28–57.
[12] O. Le Maitre, H. Najm, R. Ghanem, O. Knio, Multi-resolution analysis of Wiener-type uncertainty propagation schemes, J. Comput. Phys. 197 (2004) 502–531.

[13] M. Loève, Probability Theory, Fourth ed., Springer-Verlag, 1977.
[14] Ch. Schwab, R.A. Todor, Sparse finite elements for elliptic problems with stochastic data, Num. Math. 95 (2003) 707–734.
[15] Ch. Schwab, R.A. Todor, Karhunen–Loève approximation of random fields by generalized fast multipole methods, J. Comput. Phys. 217 (2006) 100–122.
[16] S.A. Smolyak, Quadrature and interpolation formulas for tensor products of certain classes of functions, Soviet Math. Dokl. 4 (1963) 240–243.
[17] P. Spanos, R.G. Ghanem, Stochastic finite element expansion for random media, ASCE J. Eng. Mech. 115 (5) (1989) 1035–1053.
[18] G. Szegö, Orthogonal Polynomials, American Mathematical Society, Providence, RI, 1939.
[19] M.A. Tatang, W.W. Pan, R.G. Prinn, G.J. McRae, An efficient method for parametric uncertainty analysis of numerical geophysical model, J. Geophy. Res. 102 (1997) 21925–21932.
[20] X. Wan, G.E. Karniadakis, An adaptive multi-element generalized polynomial chaos method for stochastic differential equations, J. Comput. Phys. 209 (2) (2005) 617–642.
[21] N. Wiener, The homogeneous chaos, Am. J. Math. 60 (1938) 897–936.
[22] D. Xiu, Efficient collocational approach for parametric uncertainty analysis, Commun. Comput. Phys. 2 (2) (2007) 293–309.
[23] D. Xiu, J.S. Hesthaven, High-order collocation methods for differential equations with random inputs, SIAM J. Sci. Comput. 27 (3) (2005) 1118–1139.
[24] D. Xiu, G.E. Karniadakis, Modeling uncertainty in steady state diffusion problems via generalized polynomial chaos, Comput. Methods Appl. Math. Eng. 191 (2002) 4927–4948.
[25] D. Xiu, G.E. Karniadakis, The Wiener–Askey polynomial chaos for stochastic differential equations, SIAM J. Sci. Comput. 24 (2) (2002) 619–644.
[26] D. Xiu, G.E. Karniadakis, Modeling uncertainty in flow simulations via generalized polynomial chaos, J. Comput. Phys. 187 (2003) 137–167.
[27] D. Xiu, G.E. Karniadakis, A new stochastic approach to transient heat conduction modeling with uncertainty, Inter. J. Heat Mass Trans. 46 (2003) 4681–4693.
[28] D. Xiu, S.J. Sherwin, Parametric uncertainty analysis of pulse wave propagation in a model of a human arterial networks, J. Comput. Phys. 226 (2007) 1385–1407.